

Relativistic inverse Compton scattering of photons from the early universe

S. Malu^{1*}, A. Datta^{1,3}, S. Colafrancesco², P. Marchegiani², R. Subrahmanyan⁴,
D. Narasimha⁵, M. H. Wieringa⁶

¹Centre of Astronomy, Indian Institute of Technology Indore, Simrol, Khandwa Road, Indore 453552, India

²School of Physics, University of the Witwatersrand, Private Bag 3, WITS-2050, Johannesburg, South Africa

³Center for Astrophysics and Space Astronomy, Department of Astrophysical and Planetary Science, University of Colorado, Boulder, CO 80309, USA

⁴Raman Research Institute, CV Raman Avenue, Bangalore 560080, India

⁵Tata Institute of Fundamental Research, Homi Bhabha Road, Mumbai 400005, India

⁶Australia Telescope National Facility, CSIRO Astronomy and Space Science, P.O. Box 76, Epping NSW 1710

24 May 2017

ABSTRACT

Electrons at relativistic speeds, diffusing in magnetic fields, cause copious emission at radio frequencies in both clusters of galaxies and radio galaxies, through the non-thermal radiation emission called synchrotron. However, the total power radiated through this mechanism is ill constrained, as the lower limit of the electron energy distribution, or low-energy cutoffs, for radio emission in galaxy clusters and radio galaxies have not yet been determined. This lower limit, parametrized by the lower limit of the electron momentum – p_{\min} – is critical for estimating the energetics of non-thermal electrons produced by cluster mergers or injected by radio galaxy jets, which impacts the formation of large-scale structure in the universe, as well as the evolution of local structures inside galaxy clusters.

The total pressure due to the relativistic, non-thermal population of electrons is critically dependent on p_{\min} , making the measurement of this non-thermal pressure a promising technique to estimate the electron low-energy cutoff. We present here the first unambiguous detection of this pressure for a non-thermal population of electrons in a radio galaxy jet/lobe, located at a significant distance away from the center of the Bullet cluster of galaxies.

1 INTRODUCTION

Galaxy clusters, the largest gravitationally bound structures in the universe, host large populations of hot plasma – electrons – at temperatures of up to 10–100 million Kelvins. A fraction of these galaxy clusters also host energetic population of relativistic electron plasma whose nature is still unknown. Possible sources have been proposed in relation with the existence of intra-cluster shock waves, the injection processes from radio and active galaxies and dark matter annihilation/decay. Once these relativistic electrons are produced by one or a combination of these mechanisms, they diffuse in the magnetized cluster atmosphere and emit non-thermal synchrotron radio emission observed as both extended arches and filamentary structures (named radio relics) or in more homogeneously diffuse halos (name radio halos).

A significant/critical issue in the study of non-thermal electrons through synchrotron emission is the energy distribution of these accelerated particles. Basic parameters that characterize the energy distribution of the electrons in the atmospheres of the galaxy cluster are the high- and low-energy cutoffs.

Since the energy spectrum of synchrotron emission pro-

duced by the accelerated electrons in clusters is expected to follow a power law whose intensity decreases with increasing energy/frequency, therefore, it is the low-energy cutoff that is crucial for determining the total energetics of the cluster-wide radio emission.

Radio emission from jets of radio galaxies is also due to synchrotron emission of relativistic electrons, and therefore also has a power law, and the low-energy cutoff is similarly a critical quantity to determine the energetics of the radio jets associated with these radio galaxies.

Both thermal and non-thermal populations of electrons in galaxy clusters, as well as the mostly non-thermal populations of electrons in the jets of radio galaxies, are energetic enough to cause photons, traveling from the early universe (the Cosmic Microwave Background or CMB), to shift to higher energies, hence shifting the entire CMB spectrum of photons. This is due to the fundamental mechanisms of inverse Compton scattering (ICS) and it is usually referred to as the Sunyaev–Zel’dovich Effect (or SZ Effect) for the up-scattering produced by thermal populations of electrons. Due to the universality of the ICS mechanisms, also non-thermal and relativistic electrons in galaxy clusters can up-scatter the CMB photons by largely increasing their

final frequency. This leads to a more general form of the SZ Effect that we refer to as non-thermal SZE for simplicity.

The SZ Effect probes the integrated pressure (or energy density) of the relative electron population (thermal or non-thermal) in galaxy clusters, along the line of sight – and this property renders it a critical probe of the plasma in these cosmic structures, since it yields information complementary to radio emission from synchrotron. While radio emission from synchrotron provides information about the presence of non-thermal electrons embedded in magnetic fields, the SZ Effect provides a “snapshot” of their pressure profiles; in particular, pressure enhancements, along shocks, radio galaxy jets and other regions in galaxy clusters; especially mergers or collisions of these galaxy clusters.

2 THE ‘BULLET’ CLUSTER OF GALAXIES

A spectacular example of an extremely energetic merger or collision of clusters of galaxies is the ‘Bullet’ cluster (1E0657–56), a southern sky object, named due to the eponymous shape of the smaller cluster. This cluster merger provided the most direct evidence for the existence of the so-called Dark Matter (Clowe et al. 2006), which was found to be significantly displaced with respect to X-ray emission – this is also one of the most X-ray luminous clusters observed. Other reasons that make this cluster rich in non-equilibrium physics, and one of the most interesting objects to study, are: the existence of a strong radio halo (Liang et al. 2000; Shimwell et al. 2014) which can be observed up to cm-wavelengths (Malu & Subrahmanyan 2011), a bright radio relic Shimwell et al. (2015) which has been observed up to 10 GHz (Malu et al. 2016; Shimwell et al. 2015), and the presence of a thermal SZE (Halverson et al. (2009), Plagge et al. (2010) and references therein). We present here the first unambiguous detection of the non-thermal SZ Effect in a radio galaxy jet/lobe, which is ~ 800 kpc away from the center of the Bullet cluster of galaxies. Importantly, we use low-frequency radio data in the range (2.1-9.0) GHz to determine the spectrum of the radio lobe and then fit the ATCA 18 GHz SZE observation with a non-thermal SZE model that is computed in a fully relativistic approach.

Throughout the paper, we use a flat, vacuum-dominated cosmological model with $\Omega_m = 0.315$, $\Omega_\Lambda = 0.685$ and $H_0 = 67.3 \text{ km s}^{-1} \text{ Mpc}^{-1}$.

3 THE RADIO GALAXY RG01

The Bullet cluster was observed using the Australia Telescope Compact Array (ATCA) at 18 GHz center frequency (16–20 GHz range), using the two most compact arrays, H75 and H168. Details of the observations that are used to image the SZE are provided in Malu & Subrahmanyan (2011), and in Table 1.

RG01 is one of the radio galaxies detected in the Bullet cluster field at frequencies 2.1, 5.5, 9.0 and 16–24 GHz in

Table 1. Summary of the ATCA observations

Co-ordinates (J2000) RA – Dec	06 ^h 58 ^m 14.3 ^s – 55°54′24″
Primary Beam FWHM	2.6′
Synthesized Beam FWHM:	
22.6″ × 15.9″ Natural Weighting	(Without Antenna 6)
15.7″ × 12.3″ Natural Weighting	(With Antenna 6)
7.7″ × 5.9″ Uniform Weighting	(With Antenna 6)
19.5″ × 13.8″ Uniform Weighting	(Without Antenna 6)
Frequency Range	16–20 GHz
Total observing time	140 hours
Arrays	H168 & H75
Amplitude Calibrator	PKS B1934–638
Phase Calibrator	PKS B0742–56
Frequency Resolution	1 MHz
Sensitivity	4.0 $\mu\text{Jy beam}^{-1}$
Pointings	2 (2009 observations)
	4 (2010 observations)

ATCA observations. The radio galaxy RG01 – and therefore its radio jet/lobe – is located approximately 180″ or ≈ 800 kpc away from the center of the Bullet cluster. The radio galaxy, and the jet/lobe region, is also approximately 160″, or ≈ 700 kpc away from the nearest radio halo region with diffuse radio emission, which is detected up to 10 GHz (Malu et al. 2016; Shimwell et al. 2015). In addition, there is no detectable X-ray emission with Chandra in this region. These facts (i.e., the large distance between RG01 and the center of the Bullet cluster, the absence of X-ray emission, the region containing RG01 being far away from the shock front as well as the cold front, and the SZE being in the radio jet/lobe region where synchrotron has already been detected at 2.1, 5.5 and 9.0 GHz) imply that the SZE we detect can only be of non-thermal origin.

3.1 The non-thermal SZE in the RG01 lobe

We detected a non-thermal SZE signal in the jet/lobe of the radio galaxy RG01 located at coordinates (J2000)RA: 06^h58^m14.2^s DEC: –55°54′25″ and shown in the blue-colored region of Fig. 1. Given the noise rms of 4 $\mu\text{Jy beam}^{-1}$, this is a 5.5 σ detection, with the deepest SZE signal being $-22\mu\text{Jy beam}^{-1}$. We produced images with the five different values of the FWHM, with different weightings, and different amounts of uv-coverages, as reported in Table 1. With these different weighting schemes, as well as different FWHMs of synthesized beams, the size of the two SZE regions turns out to be at most 5% different and thus retain the same morphology. Given that the natural and uniform weighing schemes provide different/independent beams, any detection above 3–5 σ that does not depend on the weighing scheme (and therefore on the deconvolution process), is therefore considered as a signal. This demonstrates that our detection of the non-thermal SZE in this region is robust. Additionally, the effect of the synthesized side-lobes is at maximum of 2% at these angular distances away from the brightest sources, assuming that it is 3′ away. Conversion from brightness to temperature units is given by $T = \frac{\lambda^2}{2k\Omega} S$ and, given that $\lambda = 1.67 \text{ cm}$ (i.e., 18 GHz), we obtain $T = 1.19 \times B$ where B is in units of $\frac{\text{Jy}}{\text{arcmin}^2}$. Since the non-thermal SZE we have shown is taken from

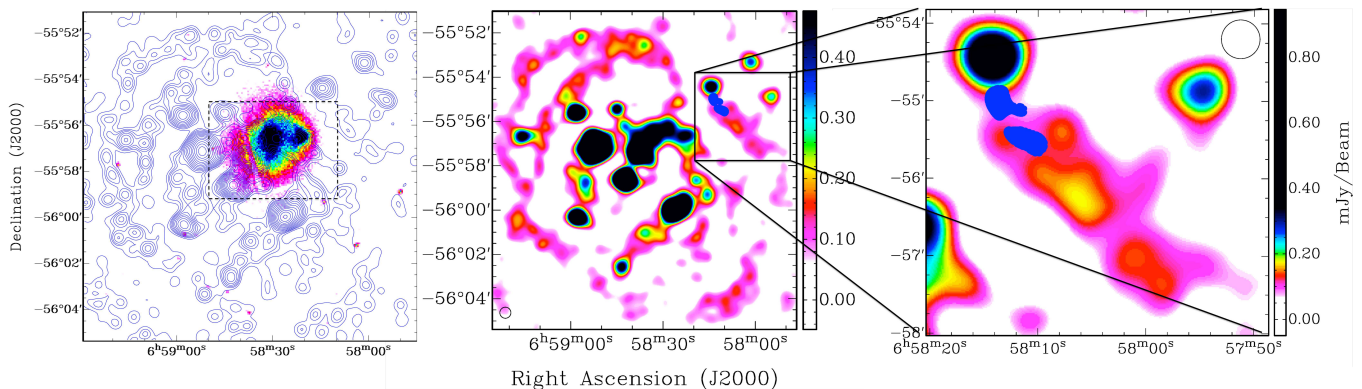


Figure 1. **Left:** 5.5 GHz contours on X-ray colour, showing the relative position of RG01 and the X-ray emission in the Bullet cluster. X-ray data was obtained from the Chandra Data Archive (500ks observations described in Markevitch (2006)), and was displayed using the KARMA package (Gooch 1996). Radio contour levels start at 5σ and increase by a factor of $\sqrt{2}$. The position and relative size of the image in Fig. 1 of Clowe et al. (2006) have been indicated and marked. This comparison clearly indicates the significantly larger spread of non-thermal emission in radio as compared to the thermal X-ray emission. **Middle:** the non-thermal SZE detected in the radio galaxy lobe/jet at 18 GHz, displayed as a blue region in the NW region of the 5.5 GHz ATCA image, with $30''$ resolution. The SZE region in blue is from an image with the same resolution of $30''$, having been convolved with a $30''$ beam. The 5.5 GHz image has a noise rms of $14\mu\text{Jy beam}^{-1}$, and the 18 GHz image has a noise rms of $3.5\mu\text{Jy beam}^{-1}$. A $30''$ beam size is represented in the bottom left corner. **Right:** a zoom-in to the region marked with a rectangle on the left image; the non-thermal SZE is marked in blue, and two distinct regions can clearly be seen, one closer to the radio galaxy core than the other. The $30''$ beam is marked in the top right corner. The colour scheme for the 5.5 GHz image is somewhat different, to accentuate small-scale features at 5.5 GHz. To the NW of the radio galaxy and radio lobe/jet there is another radio galaxy, and to the SE is the NW tip of the radio halo at 5.5 GHz, which helps mark the location of the non-thermal SZE in relation to the radio halo.

an image with a beam of $30'' \times 30''$, our detection of this SZE at $-22\mu\text{Jy beam}^{-1}$ corresponds, therefore, to $-88\mu\text{Jy arcmin}^{-2}$; from the formula in the previous equation this yields $\Delta T_{\text{SZ}} = -105\mu\text{K}$, and a Compton-y parameter of $y = -\frac{1}{2} \frac{\Delta T_{\text{SZ}}}{T_{\text{CMB}}} = 1.9 \times 10^{-5}$.

4 MODELING THE NON-THERMAL SZ EFFECT

We model the non-thermal SZE signal we detected in the RG01 lobe using a full relativistic formalism (Colafrancesco et al. 2003), where the SZE spectrum is given by the expression $\Delta I(x) = I(x) - I_0(x)$. The incoming radiation spectrum is the CMB spectrum $I_0(x) = 2 \frac{(kT_0)^3}{(hc)^2} \frac{x^3}{e^x - 1}$, with $x = h\nu/kT_0$ and T_0 is the CMB temperature today. The resulting SZE spectrum is calculated according to the equation $I(x) = \int_{-\infty}^{+\infty} I_0(xe^{-s})P(s)ds$, where $P(s)$ is the photon redistribution function (yielding the probability of a logarithmic shift $s = \ln(\nu'/\nu)$ in the photon frequency due to the inverse Compton scattering process) that depends on the electron spectrum producing the CMB Comptonization, and includes all the relativistic corrections. It is calculated by the sum of the probability functions to have n scatterings, $P_n(s)$, weighted by the corresponding Poissonian probability: $P(s) = \sum_{n=0}^{+\infty} \frac{e^{-\tau} \tau^n}{n!} P_n(s)$, where the optical depth τ is given by the integral along the line of sight ℓ of the electron density $\tau = \sigma_T \int n_e dl$, where n_e is the electron plasma density. Each function $P_n(s)$ is given by the convolution product

of n single scattering probability functions $P_1(s)$:

$$P_n(s) = \underbrace{P_1(s) \otimes \dots \otimes P_1(s)}_{n \text{ times}} \text{ where } P_1(s) = \int_0^\infty f_e(p)P_s(s,p)dp,$$

and where $f_e(p)$ is the electron momentum distribution function (normalized as to have $\int_0^\infty f_e(p)dp = 1$), and $P_s(s,p)$ is the function that gives the probability to have a frequency shift s by an electron with a-dimensional momentum $p = \beta\gamma$, and is given by the physics of the inverse Compton scattering process (see, e.g., Colafrancesco et al. (2003); Enßlin & Kaiser (2000)).

For non-thermal electrons we use a single power-law electrons momentum distribution with a minimum momentum p_1
 $f_e(p) \propto p^{-s_e}$; $p_1 \leq p \leq p_2$,
 and we assume a high value of the maximum momentum ($p_2 = 10^8$).

Our 18 GHz observation for the RG01 SZE signal can be fitted, in principle, with both a thermal or a non-thermal electron population with different values of the spectral index and the minimum momentum of electrons (for the non-thermal SZE) and of the temperature (for the thermal SZE), leaving the optical depth as a free parameter: this is, in fact, the result of a degeneracy in the SZE parameters at low-frequencies. However, the absence of any detectable X-ray emission in this region, its large distance from the centre of the cluster merger (≈ 800 kpc), and the absence of any diffuse emission in a region roughly 400 kpc region E to W from the westernmost edge of X-ray emission, imply that emission observed in this region does not have a thermal origin.

In order to break this parameter degeneracy, we obtained information about the spectral index of the electrons in the

RG01 lobe from the observed radio spectrum at frequencies in the range 2.1-9.0 GHz: the average radio spectral index measured between 2.1 and 9 GHz is $\alpha_r = 1.1 \pm 0.15$. This corresponds to a range of electrons spectral index values in the range $2.9 \leq s_e \leq 3.5$, where $s_e = 2\alpha_r + 1$. The shape of the radio spectrum indicates that we are in the presence of a quite typical non-thermal electron distribution in the RG01 lobe; this important fact allows us to constrain the range of possible SZE models that can fit the observed SZE signal at 18 GHz, thus restricting our analysis to non-thermal models of the SZE.

Fig. 2 reports the non-thermal SZE in the RG01 lobe calculated with the value of the average radio spectral index measured between 2.1 and 9 GHz $\alpha_r = 1.1$ corresponding to $s_e = 3.2$ and is shown at low frequencies ($\nu < 50$ GHz), at high frequencies ($\nu < 1000$ GHz), as well as the ICS X-ray emission expected for several values of the minimum momentum p_1 of the non-thermal electron distribution. All the non-thermal SZE models which are consistent with the observed radio spectrum of the RG01 lobe can fit the ATCA SZE signal at 18 GHz confirming that the SZE signal we detected is of non-thermal origin and it is produced by a non-thermal electron population whose energy spectrum is consistent with the observed radio synchrotron spectrum. This is the first detection of a non-thermal SZE effect in the lobe of a radio galaxy. The upper limit on X-ray emission from the RG01 lobes provided by Chandra indicates an upper limit on the value of p_1 between 5 and 10 that correspond to minimum electron energies $E_{\min} < 2.5 - 5$ MeV.

The central panel of Fig.3 shows that a more precise determination of the value of p_1 can be obtained by measuring the spectrum of the non-thermal SZE at high frequencies, i.e. at the crossover frequency, that can vary between ~ 250 and ~ 500 GHz depending on the value of p_1 , or in the high energy part of the spectrum, where the SZE is positive. This is in agreement with previous studies of the properties of non-thermal electrons in radio galaxy lobes from SZE measurements (see Colafrancesco & Marchegiani (2011)). We note that a measurement of p_1 can lead to an estimation of the optical depth τ , and this value in turn leads to crucial information about the physics of radio galaxy lobes; namely, density of non-thermal electrons and the intensity of the magnetic field in the lobe (see discussion in Colafrancesco & Marchegiani (2011)).

5 CONCLUSIONS

The first detection of the non-thermal SZE presented here in a radio galaxy jet, after its theoretical prediction (see Colafrancesco (2008)), is a significant step towards the characterization of the low-energy cut-off in a non-thermal plasma, and its usefulness and importance therefore cut across several fields in astrophysics. Extension of the non-thermal SZE observed in the lobe of RG01 at higher frequencies can also be observed with mm and sub-mm experiments with appropriate sensitivity and angular resolution (like ALMA and Millimetron).

Future detection of X-ray emission from the same physical process, i.e. the up-scattering of CMB photons by non-thermal populations of electrons in the lobe of RG01, combined with radio and SZ Effect, will provide a value of the

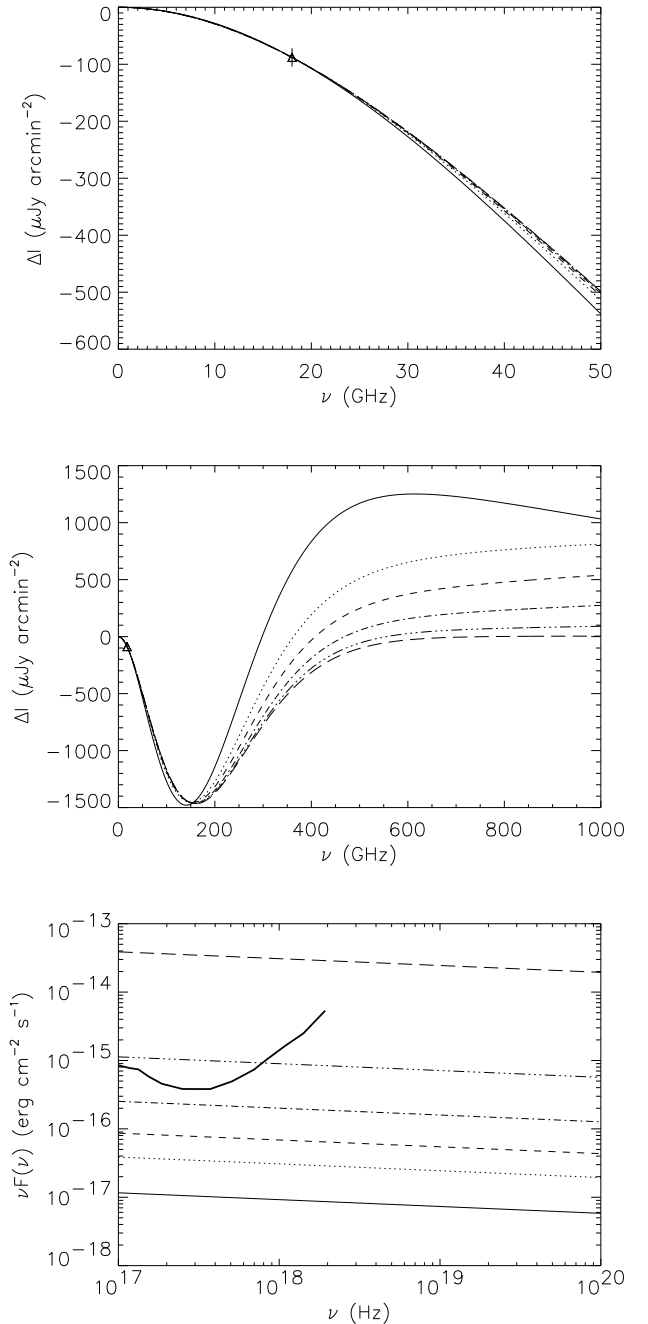


Figure 2. Spectrum of the **non-thermal SZE** (in surface brightness units) at low (upper panel) and high frequencies (middle panel) and of the ICS emission in the X-rays integrated inside a square with side length of 4 arcsec (lower panel) for an electrons non-thermal population with $s_e = 3.2$. The following models are plotted: solid line: non-thermal SZE with minimum momentum of electrons $p_1 = 1$ and optical depth $\tau = 7.6 \times 10^{-5}$; dotted line: $p_1 = 2$ and $\tau = 5.5 \times 10^{-5}$; dashed line: $p_1 = 3$ and $\tau = 5.1 \times 10^{-5}$; dot-dashed line: $p_1 = 5$ and $\tau = 4.8 \times 10^{-5}$; three dots-dashed line: $p_1 = 10$ and $\tau = 4.7 \times 10^{-5}$; long-dashed line: $p_1 = 50$ and $\tau = 4.6 \times 10^{-5}$. The sensitivity of Chandra is plotted for an integration time of 100 ks (Takahashi et al. 2012).

overall energy extension and spectral shape of the energy spectrum of these non-thermal electrons residing in lobes of radio galaxies.

ACKNOWLEDGEMENTS

The Australia Telescope Compact Array is part of the Australia Telescope which is funded by the Commonwealth of Australia for operation as a National Facility managed by CSIRO. X-ray data was obtained from the Chandra Data Archive, observations made by the Chandra X-ray Observatory and published previously in cited articles. The radio / X-ray overlay image was made using the KARMA package (Gooch 1996). Observations and analysis were made possible by a generous grant for Astronomy by IIT Indore, and travel funding for S.M. by RRI, Bangalore and IIT Indore. S.C. acknowledges support by the South African Research Chairs Initiative of the Department of Science and Technology and National Research Foundation (Grant No 77948) and by the Square Kilometre Array (SKA). P.M. acknowledges support from the DST/NRF SKA post-graduate bursary initiative.

REFERENCES

- Clowe, D., Bradac, M., Gonzalez, A. H., Markevitch, M., Randall, S. W., Jones, C., & Zaritsky, D. 2006, *ApJ*, 648, L109
- Colafrancesco, S. 2008, *MNRAS*, 385, 2041
- Colafrancesco, S., & Marchegiani, P. 2011, *A&A*, 535, A108
- Colafrancesco, S., Marchegiani, P., & Palladino, E. 2003, *A&A*, 397, 27
- Enßlin, T. A., & Kaiser, C. R. 2000, *A&A*, 360, 417
- Gooch, R. 1996, in *Astronomical Society of the Pacific Conference Series*, Vol. 101, *Astronomical Data Analysis Software and Systems V*, ed. G. H. Jacoby & J. Barnes, 80
- Halverson, N. W., et al. 2009, *ApJ*, 701, 42
- Liang, H., Hunstead, R. W., Birkinshaw, M., & Andreani, P. 2000, *ApJ*, 544, 686
- Malu, S., Datta, A., & Sandhu, P. 2016, *Ap&SS*, 361, 255
- Malu, S. S., & Subrahmanyan, R. 2011, *Journal of Astrophysics and Astronomy*, 32, 541
- Markevitch, M. 2006, in *ESA Special Publication*, Vol. 604, *The X-ray Universe 2005*, ed. A. Wilson, 723
- Plagge, T., et al. 2010, *ApJ*, 716, 1118
- Shimwell, T. W., Brown, S., Feain, I. J., Feretti, L., Gaensler, B. M., & Lage, C. 2014, *mnras*, 440, 2901
- Shimwell, T. W., Markevitch, M., Brown, S., Feretti, L., Gaensler, B. M., Johnston-Hollitt, M., Lage, C., & Srinivasan, R. 2015, *mnras*, 449, 1486
- Takahashi, T., et al. 2012, in *Proc. SPIE*, Vol. 8443, *Space Telescopes and Instrumentation 2012: Ultraviolet to Gamma Ray*, 84431Z